Distinguishing forest types in restored tropical landscapes with UAV-borne LIDAR

Janneke Scheeres [a,b], Johan de Jong [a,b,*], Benjamin Brede [b,c], Pedro H.S. Brancalion [d], Eben Noth Broadbent [e], Angelica Maria Almeyda Zambrano [f], Eric Bastos Gorgens [g], Carlos Alberto Silva [h], Ruben Valbuena [i], Paulo Molin [j], Scott Stark [k], Ricardo Ribeiro Rodrigues [d], Giulio Brossi Santoro [d], Angélica Faria Resende [d], Catherine Torres de Almeida [d], Danilo Roberti Alves de Almeida [d]

[a] *Wageningen University & Research, Forest Ecology and Forest Management, Droevendaalsesteeg 3, 6708 PB Wageningen, the Netherlands*
[b] *Wageningen University & Research, Laboratory of Geo-Information Science and Remote Sensing, Droevendaalsesteeg 3, 6708 PB Wageningen, the Netherlands*
[c] *Helmholtz Center Potsdam GFZ German Research Centre for Geosciences, Section 1.4 Remote Sensing and Geoinformatics, Telegrafenberg, 14473 Potsdam, Germany*
[d] *Department of Forest Sciences, "Luiz de Queiroz" College of Agriculture, University of São Paulo (USP/ESALQ), Piracicaba, SP, Brazil*
[e] *Spatial Ecology and Conservation (SPEC) Lab, School of Forest, Fisheries, and Geomatics Sciences, University of Florida, Gainesville, FL 32611, USA*
[f] *Spatial Ecology and Conservation (SPEC) Lab, Center for Latin American Studies, University of Florida, Gainesville, FL 32611, USA*
[g] *Department of Forest Engineering, Universidade Federal dos Vales do Jequitinhonha e Mucuri, Diamantina, MG CEP 39100-000, Brazil*
[h] *Forest Biometrics and Remote Sensing Lab (Silva Lab) - School of Forest Resources and Conservation, University of Florida, Gainesville, FL 32611, USA*
[i] *Forest Remote Senisng Division, Department of Forest Resource Management, Swedish University of Agricultural Sciences, SLU Skogsmarksgränd 17, SE-901 83 Umeå, Sweden*
[j] *Center for Nature Sciences, Federal University of São Carlos, Buri, SP CEP 18290-000, Brazil*
[k] *Department of Forestry, Michigan State University, East Lansing, MI 48824, USA*

ARTICLE INFO

ABSTRACT

Forest landscape restoration is a global priority to mitigate negative effects of climate change, conserve biodiversity, and ensure future sustainability of forests, with international pledges concentrated in tropical forest regions. To hold restoration efforts accountable and monitor their outcomes, traditional strategies for monitoring tree cover increase by field surveys are falling short, because they are labor-intensive and costly. Meanwhile remote sensing approaches have not been able to distinguish different forest types that result from utilizing different restoration approaches (conservation versus production focus). Unoccupied Aerial Vehicles (UAV) with light detection and ranging (LiDAR) sensors can observe forests` vertical and horizontal structural variation, which has the potential to distinguish forest types. In this study, we explored this potential of UAV-borne LiDAR to distinguish forest types in landscapes under restoration in southeastern Brazil by using a supervised classification method. The study area encompassed 150 forest plots with six forest types divided in two forest groups: conservation (remnant forests, natural regrowth, and active restoration plantings) and production (monoculture, mixed, and abandoned plantations) forests. UAV-borne LiDAR data was used to extract several Canopy Height Model (CHM), voxel, and point cloud statistic based metrics at a high resolution for analysis. Using a random forest classification model we could successfully classify conservation and production forests (90% accuracy). Classification of the entire set of six types was less accurate (62%) and the confusion matrix showed a divide between conservation and production types. Understory Leaf Area Index (LAI) and the variation in vegetation density in the upper half of the canopy were the most important classification metrics. In particular, LAI understory showed the most variation, and may help advance ecological understanding in restoration. The difference in classification success underlines the difficulty of distinguishing individual forest types that are very similar in management, regeneration dynamics, and structure. In a restoration context, we showed the ability of UAV-borne LiDAR to identify complex forest structures at a plot scale and identify groups and types widely distributed across different restored landscapes with medium to high accuracy. Future research may explore a

* Corresponding author at: Wageningen University & Research, Forest Ecology and Forest Management, Droevendaalsesteeg 3, 6708 PB Wageningen, the Netherlands.
E-mail address: johandejong@protonmail.com (J. de Jong).

fusion of UAV-borne LiDAR with optical sensors, and include successional stages in the analyses to further characterize and distinguish forest types and their contributions to landscape restoration.

1. Introduction

Forest restoration has become increasingly important to reverse forest cover losses and forest degradation. There are global ambitions to restore 3.5 million km² of forests, especially in tropical regions where population densities are low, many areas are degraded, and the potential for biodiversity conservation and climate change mitigation is high (Brancalion et al., 2019). A portfolio of restoration strategies is being used depending on local opportunities, site conditions, and needs (Chazdon et al., 2016). These strategies may either have a stronger conservation focus (e.g. by focusing on remnant forests, natural regrowth or active restoration plantings) or a stronger production focus (e.g. by focusing on monoculture plantations, mixed plantations, or abandoned plantations) (Hua et al., 2022). The balance between conservation and production forests in restoration initiatives has been an important controversy, as established and planned production forests with exotic tree species predominate in many global regions (Lewis et al., 2019). Until now tree cover loss and gain has been the central indicator used to evaluate restoration and reforestation advancement at large scales (Nanni et al., 2019), but it has critical limitations to understanding how restoration has been implemented and for estimating its potential benefits to nature and people (Marshall et al., 2022). In the context of the unprecedented scale of forest restoration and monitoring their outcomes, distinguishing between these restoration approaches and establishing a baseline for monitoring their outcomes is a first step towards a more meaningful accountability of these restoration initiatives. Here, we evaluate the potential of Unoccupied Aerial Vehicles equipped with Light and Detection Ranging (UAV-LiDAR) to distinguish between six different tropical forest restoration types based on their structural attributes and leaf area components with supervised classification.

1.1. Different restoration types

Different forest restoration approaches can be used to match project objectives in varying socio-ecological conditions (Fig. 1). For instance, restoring native forest functions, by means of natural regeneration or restoration plantations, maximizes biodiversity conservation and key ecosystem services (e.g. carbon storage, soil erosion control, water provisioning) compared to exotic tree plantations, but results in lower contribution to wood supply (Hua et al., 2022). Mixed and abandoned plantations provide higher environmental benefits than monoculture tree plantations (Feng et al., 2022). Furthermore, active management in plantations, including the removal or suppression of understory vegetation and the planting of trees in rows, leads to different forest structures than in naturally regenerated forests (Chazdon and Guariguata, 2016). Regarding native forests, natural regeneration is advantageous because it is cheaper, more scalable, and maximizes biodiversity recovery compared to mixed plantations of native trees (Chazdon et al., 2020; Crouzeilles et al., 2017), but this restoration approach is unsuitable for more degraded areas, with lower resilience (Holl and Aide, 2011). As landscapes undergoing forest restoration are often a heterogeneous mosaic of different restoration approaches, with different ages, species composition, and management, qualifying the restored tree cover is crucial, yet underdeveloped in technical terms.

1.2. The importance of forest structure

Forest structure is an important indicator for forest functioning and ecosystem processes (Poorter et al., 2021; Zolkos et al., 2013). For example, structural attributes (e.g. leaf area index (LAI), height, and basal area) are main drivers of carbon storage and accumulation, which are critical attributes for climate change mitigation (Lohbeck et al., 2015; van der Sande et al., 2017; Almeida et al., 2019a). In contrast to species diversity, structural attributes are less sensitive to sampling area,

Production

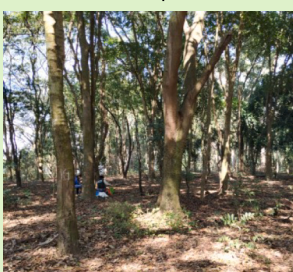Monoculture plantation   Abandoned monoculture   Mixed plantation

Conservation

Restoration plantation   Second-growth forest   Forest remnant
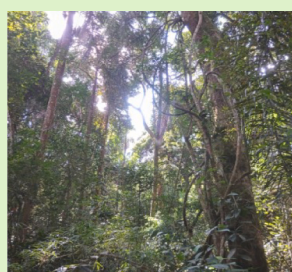
Fig. 1. New forest types that result from different restoration approaches. These six types are included in this study. Monoculture plantations consist of a single tree species, abandoned monoculture consists of a single tree species with naturally regenerating understory, mixed plantations consist of two or a few commercial tree species, restoration plantations consist of mixed plantations of several native tree species, second-growth forests consist of spontaneous recolonization of tree species, forest remnants consist of mostly disturbed and fragmented old-growth forest.

and hence, monitoring structural attributes has more potential for restoration outcomes (Chazdon et al., 2022; Marshall et al., 2022). Also, increased forest structure, including height and height variation, is associated with higher species diversity, because of increased complexity in the canopy and biomass and vertical niche occupation (Almeida et al., 2021; Marselis et al., 2019). LAI, which is the one-sided leaf area per unit ground area, is an important feature, because the total leaf area plays a critical role in forest primary production, nutrient cycles, and respiration (Asner et al., 2003; Clark et al., 2008; Fang et al., 2019). Therefore, monitoring forest structure with UAV-LiDAR can be a viable, integrative strategy to operationalize the indirect assessment of forest diversity and functioning at larger scales.

1.3. Need to upscale monitoring across space and time using remote sensing

Forest monitoring is traditionally done using conventional forest inventories and permanent sample plots. However, with the global ambitions to scale up restoration efforts, it is also important to upscale monitoring efforts across space and time (de Almeida et al., 2019). The first step to upscale these monitoring efforts is to establish a baseline of the landscapes under restoration, starting with distinguishing different restoration approaches (this study). UAVs are suitable for classifying different restoration approaches and monitoring forest restoration, because they 1) cover large areas within one flight, 2) provide high spatial resolution, and 3) give information about key ecological indicators, such as vegetation structural attributes and species identification. Multispectral technologies allow to identify species and estimate biomass and primary productivity, but have the disadvantage that many vegetation reflectance indices saturate with dense canopies, and that they cannot adequately describe forest structure. LiDAR has the ability to capture the three dimensional structure of sub-canopy layers and to accurately quantify canopy height, canopy cover, LAI, and aboveground biomass (Drake et al., 2002; Luo et al., 2019; van Leeuwen and Nieuwenhuis, 2010). UAV-LiDAR systems are light-weight, fieldportable, have a relatively low cost, can acquire imagery at fine spatial and temporal resolutions, and are more flexible in use than other LiDAR systems (Sankey et al., 2017; Zahawi et al., 2015). They are expected to revolutionize forest monitoring considering their potential for identification and monitoring of restoration forest types (Almeida et al., 2019, 2019d and 2021; Camarretta et al., 2020; Sankey et al., 2017). However, the application of UAV-borne LiDAR for monitoring in a tropical forest restoration context is relatively new (but see Almeida et al., 2019a, 2019b, 2021b).

1.4. Forest type classification for monitoring with LiDAR

Typically, tree cover classification is accomplished by using supervised machine learning algorithms in combination with multispectral images. Supervised classification with machine-learning algorithms exploded during the past two decades, because they can handle complex data structures and make no assumptions about the data distribution (Maxwell et al., 2018). Specifically the Random Forest (RF) algorithm gained in popularity because of its reliable classification results and ability to rank the importance of input variables on the classification result (Belgiu and Drăguţ, 2016). To date, however, combining UAV-LiDAR based vegetation structural attributes with supervised classification for distinguishing forest types and monitoring restoration is relatively unexplored, but is gaining momentum.

To this end, we explored the potential of UAV-LiDAR-derived structural metrics to distinguish six tropical forest restoration types that differ in their conservation and production value in landscapes undergoing restoration. More specifically, we evaluate how structural attributes are associated with tropical forest restoration types (six types and two groups based on conservation and production value) by applying supervised classification methods. We also discuss monitoring

forest restoration outcomes with UAV and LiDAR systems.

2. Methods

2.1. Study area and field data

The study areas are located in the ecotone zone between the Atlantic Forest and Cerrado in southeastern Brazil, which are considered biodiversity hotspots for conservation priorities (Myers et al., 2000). We selected four human-modified tropical landscapes that are representative for landscapes under restoration in the southeast of Brazil. These landscapes range between 4 and 10 km² each. These landscapes experienced a recent increase in tree cover resulting from the expansion of commercial tree plantations, restoration plantations, and second-growth forests (Fig. 2). Within the studied landscapes, we grouped all new forests into six different forest types, because these forest types represent a gradient of human interference on ecosystem composition, structure and functioning, and these types are increasingly expanding into the anthropized landscapes in the southeast of Brazil (Fig. 1, Table 1). The four landscapes are experimental areas of the University of São Paulo. Two landscapes are experimental stations (Anhembi and Itatinga), one landscape is an experimental farm (Areão), and one landscape is at a São Paulo university campus (ESALQ in Piracicaba) (Fig. 2). The elevation of landscapes varies between 450 and 850 m above sea level with <100 m variability within landscape. The native vegetation is mostly seasonal semi-deciduous forests, the regional climate has dry winters and wet summers, with a mean annual precipitation ranging from 1100 to 1367 mm, and mean temperatures from 20 °C to 23 °C (Köppen climate type Cwa) (César et al., 2018).

The six forest types were based on information from local partners, land use and land cover maps, and visual interpretation of satellite imagery (or products thereof, e.g. MapBiomas). The definitions of the six types in this study are (see Fig. 1 for a visual overview):

- *Monoculture plantation*: plantations of a single tree species, native or exotic, permanently managed for commercial purposes, including understory clearing.
- *Abandoned monoculture*: monoculture plantations without understory clearing, which may have allowed spontaneous recolonisation by native tree species.
- *Mixed plantation*: plantations of two or a few more commercial tree species managed for production, including understory clearing.
- *Restoration plantation*: mixed plantations of several native tree species, managed for restoring native forest ecosystems.
- *Second-growth forests*: established through the spontaneous recolonization of tree species following land abandonment, without tree planting or human assistance.
- *Remnant forests*: old-growth forests, which were mostly disturbed by fragmentation and human disturbances. They do not represent a conserved forest and might have suffered from biodiversity losses.

Next, we grouped the six types in two simplified groups: (1) conservation - remnant forests, second-growth forests, and restoration plantation, and (2) production forests - monoculture plantation, abandoned plantation, and mixed plantation (Fig. 1; Table 1).

We then established inventory plots in polygons covered by each forest type, with a size of 900 m² (30 × 30 or 20 × 45 m). We measured the Diameter Breast Height (DBH), identified all trees DBH >5 cm within each plot, and sampled the GPS positions of the four corners for each plot with a GNSS device when possible and otherwise a handheld Garmin device. Plots were separated at least 60 m from each other, and to avoid large edge effects, we located plots at least 30 m from the forest edge. Whenever possible, we avoided forested areas <1 ha. In total, 150 plots were sampled between 2018 and 2020 (Table 1). More details about summary statistics of the plots per forest type can be found in Supplementary Materials B.
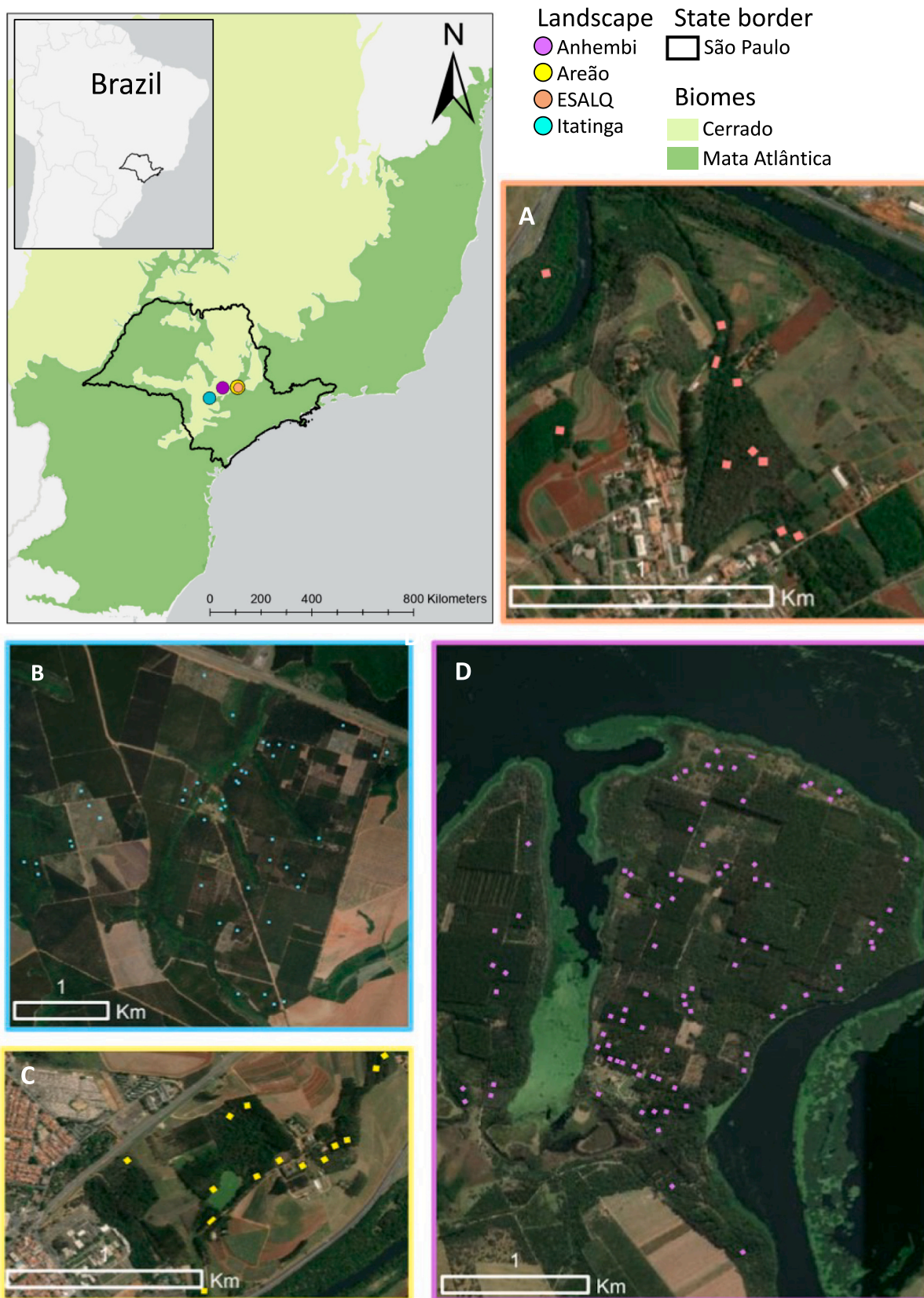
Fig. 2. Study landscapes and plots in southeastern Brazil. A, B, C, D are the landscapes ESALQ, Itatinga, Areão, and Anhembi, respectively. The colored dots represent the plots in each landscape. Map sources: Esri World Imagery; Global Forest Watch "Brazil biomes"; AmeriGEOSS datahub - Brazil subnational administrative boundaries.

Table 1
Number of sampled plots per forest type in each of the four sites.

Forest type	Areão	Anhembi	ESALQ	Itatinga	Total
Monoculture plantation	4	36	1	20	61
Abandoned monoculture	1	12	0	7	20
Mixed plantation	4	2	0	2	8
Restoration plantation	4	10	5	11	30
Second-growth forest	0	17	1	6	24
Forest remnant	1	2	3	1	7
Total					150

2.2. UAV-borne LiDAR data acquisition

We used UAV-borne LiDAR data which was acquired with the GatorEye system from the Spatial Ecology & Conservation Lab at the University of Florida, United States. The data is available on the GatorEye data access platform (http://www.speclab.org/gatoreye.html). The GatorEye system includes a vertical takeoff and landing DJI Matrice 600 Pro hexacopter. The GatorEye 'Gen 2' system contained a Phoenix Scouth computational core, which integrates a Velodyne VLP-32c dual-return laser scanner which can record up to 600,000 returns per second and has a functional range of up to 200 m as well as time-synchronized and co-aligned visual and hyperspectral sensors. The LiDAR is a discrete-return sensor that captures the strongest return (first return) and last return from each pulse, or it captures one single 'combined' strongest return if both occur simultaneously.

We collected the data per landscape in three consecutive days (27th, 28th and 29th of August 2019). Flights were conducted 100 m aboveground level and at a velocity of 10 m/s. Most flight lines overlapped >50% and each plot was covered by 2 to 4 different flight lines with an average point density of 237 points per m^2. Visual examples of point clouds of each forest type can be found in Supplementary Materials C.

2.3. UAV-borne LiDAR data processing

To calculate forest metrics from LiDAR data, we first extracted the point clouds representing the forest plots from the full flight lines with LAStools in R (Fig. 3). Next, we computed LiDAR metrics from Canopy Height Models (CHM), ground-normalized point clouds, and voxelized point clouds. We removed highly correlated metrics.

We used data from 150 field plots of 30 × 30 m. We used polygons to clip the point clouds per plot. Then, we classified ground points and interpolated with a Triangular Irregular Network (TIN) to produce the digital terrain model (DTM). Subsequently, we normalized the point clouds by replacing the elevation of each point (i.e., the z coordinate) with its height above the ground. This process produced clipped height normalized point clouds for each plot. The point density and average spacing of point clouds clipped by the locations of the plots per landscape can be found in Table 2.

We derived three types of LiDAR metrics on plot scale: Canopy Height Model (CHM) based metrics, point cloud-based statistics, and voxel-based metrics (see Table 3). The CHM and point cloud based metrics were calculated with a grid resolution of 0.25 m after which we calculated the mean and variation on plot scale. The standard deviations were calculated as follows:

$$\sigma = \sqrt{\frac{\sum (x_i - \mu)^2}{N}} \qquad (1)$$

where x_i are the values of the grid cells and μ is their average. In total, 33 metrics for all 150 plots were calculated (Table 3). We processed all data in R (R Core Team R Foundation for Statistical Computing, 2022).

First, we computed CHMs with the normalized point clouds based on the spike-free algorithm of Khosravipour et al. (2016) with a grid resolution of 0.25 m. This resolution was chosen based on the point spacing value of the point clouds with the lowest point density (see Table 2),
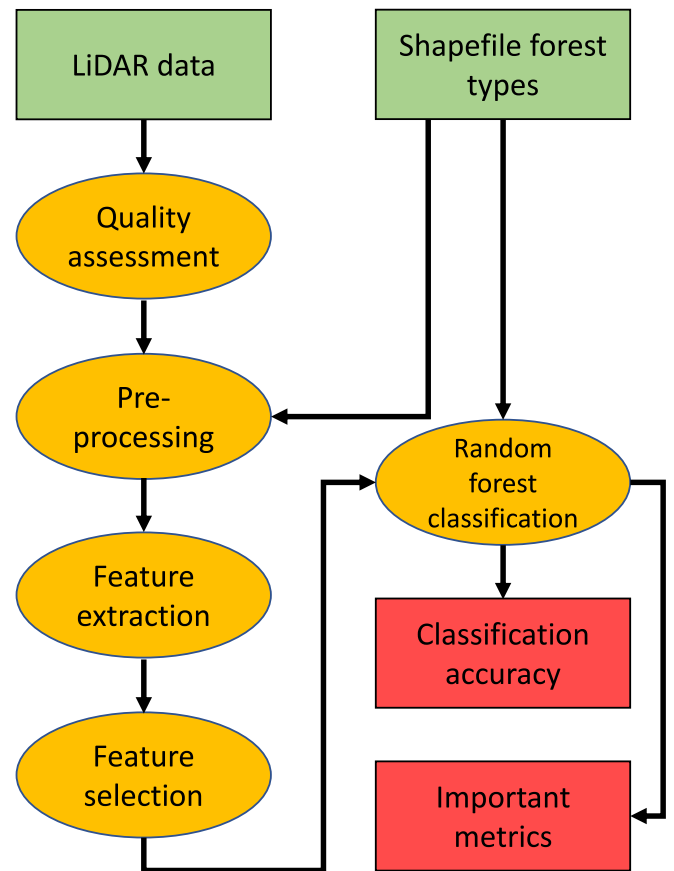

Fig. 3. General overview of the data, processes, and outcomes of the processing and analysis methodology.

Table 2
Point density and average spacing details for the processed point clouds of the four sampling areas.

Landscape	Point density (points/m^2)		Point spacing (m)	
	mean	SD	mean	SD
Anhembi	84.20	71.46	0.13	0.04
Areão	397.09	124.20	0.05	0.01
ESALQ	180.67	89.57	0.09	0.03
Itatinga	286.52	143.30	0.07	0.02

which is approximately twice the highest point spacing distance. To reduce edge effects while generating the CHM, we added a plot shapefile buffer of 10 m. Thereafter, we calculated the mean CHM per plot from the gridded height values in the plot; conceptually, this is the average tree top height above the ground (visual overview see Supplementary Materials D). Papa et al. (2020) found that this metric captured variation in forest types well and had a high correlation with basal area. Next, we calculated canopy rugosity as the standard deviation (SD) of the gridded height values. Rugosity represents the canopy heterogeneity and was a useful discriminator in forest type classification in another study (Almeida et al., 2019b). Next, we calculated the gap fraction with the ForestGapR package (Silva et al., 2019) as the fraction of cells with height values lower than 10 m and a threshold size of at least 10 m^2 (Stark et al., 2012). Gap fraction represents the canopy openness in general, and is highly correlated with the number of large openings (or forest gaps) in the forest canopy. Gap fraction is a good indicator of restoration effectiveness and commercial plantations and second-growth forests, because they can considerably differ in gap fraction (Almeida et al., 2019c). Additionally, we have identified gap fraction as

Table 3

A summary of all derived LiDAR metrics. CHM-derived metrics and point cloud statistics are calculated with a grid cell resolution of 0.25 m. Voxel-derived metrics are calculated with a grid cell resolution of 1.0 m and voxels of 1 m^3.

Metric	Definition	Reference
CHM derived ($N =$ 3)		
Mean CHM	Average of CHM	Papa et al. (2020)
Canopy rugosity	Standard deviation of CHM	Almeida et al. (2019b) and Papa et al. (2020)
Gap fraction	Fraction of CHM cells below 10 m with threshold size of 10 m^2	Almeida et al. (2019a) and Stark et al. (2012)
Point cloud statistics ($N =$ 25)		
Mean height percentile (hp_nmean)	Average height at n percentile ($n =$ 5, 10, 25, 50, 75, 90) of returns	Cao et al. (2014)
SD height percentiles (hp_nSD	Standard deviation of height at n percentile ($n = 5, 10, 25, 50, 75, 90$) of returns	Cao et al. (2014)
Mean cloud return density (dq_imean)	Average of the proportion of points above i quantile height ($i = 20, 40, 60, 80$) to total points	Cao et al. (2014) and Maltamo et al. (2005)
Variation cloud return density (dq_iSD)	Standard deviation of the proportion of points above i quantile height ($i = 20, 40, 60, 80$) to total points	Cao et al. (2014) and Maltamo et al. (2005)
Mean minimum returns (C_{min}mean)	Average of minimum height of returns	Shi et al. (2018b)
SD minimum returns (C_{min}SD)	Standard deviation of minimum height of returns	Shi et al. (2018b)
Mean maximum returns (C_{max}mean)	Average of maximum height of returns	Cao et al. (2014)
SD maximum returns (C_{max}SD)	Standard deviation of maximum height of returns	Cao et al. (2014)
Gini coefficient (GC)	L-coefficient of variation of heights	Valbuena et al. (2017)
Voxel derived (N = 5)		
LAI mean	Average of leaf area per unit ground area	Almeida et al. (2019a)
LAI SD	Standard deviation of leaf area per unit ground area	Almeida et al. (2019a)
LAI understory	Leaf area at all heights <5 m	Almeida et al. (2019b)
Leaf Area Height Volume (LAHV)	Sum of average leaf volume at each height interval over all heights	Almeida et al. (2019b)
Foliage Height Diversity (FHD)	Shannon's diversity calculated over Leaf Area Density (LAD) profiles	Stark et al. (2012)

a strong predictor of biomass growth and recruitment (Stark et al., 2012).

Second, we extracted 25 metrics directly from the normalized point clouds. For each 0.25 m grid cell, we calculated the 25 metrics and thereafter derived the plot-scale mean and SD from all grid cells within the corresponding plot. The 25 plot-scale metrics were: six mean and six SD height percentile cloud metrics hpnmean and hpnSD, where n = [5,10,25,50,75,90]; four mean and four SD cloud return density above quantile metrics dqimean and dqiSD, where i = [20,40,60,80]; mean and SD minimum return height Cminmean and CminSD; mean and SD maximum return height Cmaxm and CmaxSD; and Gini coefficient (GC) (Table 3, visual overview see Supplementary Materials D). The height percentile metrics based on the height normalized point clouds represent the distribution of vegetation through the canopy, specifically at which height a proportion of vegetation is concentrated, i.e. the mean height percentile, and the horizontal variation in that height distribution, i.e. the SD height percentile. Cao et al. (2014) used height percentiles as predictors of biomass, and found that they explained most

variability in forest structural attributes. The return density metrics represent the average (mean) and variation (SD) in vegetation density in a proportion of the canopy. Thus, these metrics can indicate whether the vegetation is most dense in the top of the canopy or is more evenly distributed. Maltamo et al. (2005) found that these density metrics could capture structural layers in heterogeneous forests and Cao et al. (2014) used them to predict structural attributes. Minimum return heights above the estimated ground surface at the plot level are influenced by the presence and variation of vegetation beneath the canopy: low mean values indicate a continuous cover of understory vegetation, while higher values indicate a more open, and likely more heterogeneous, understory. Maximum return heights indicate the canopy height (mean) and variation in canopy height. These were used by Shi et al. (2018a) as individual tree characteristics to identify tree species. GC is a measure of inequality, which can capture height inequality variation in forest stands. Valbuena et al. (2016) used the GC to emphasize differences in forests created by different management.

We calculated the height percentile metrics as the plot mean and SD of the height at n% of the returns of all grid cells (n = [5,10,25,50,75,90]). We calculated the return density metrics as the plot mean and SD of the density fraction of all cells as the portion of returns above the quantiles (i = [20,40,60,80]) divided by the total number of returns. We calculated the minimum and maximum returns as the plot mean and SD of the height at the minimum or maximum returns of all grid cells. We calculated GC with the leafR package (Almeida, 2021a) following the variation by Valbuena et al. (2017), who used the L-coefficient of variation. This coefficient is computed with L-moments, which are order statistics of probability density distributions (Valbuena et al., 2017). It was calculated as the ratio between the L-moment analogous to standard deviation and the L-moment analogous to mean.

Third, we calculated five voxel-based metrics based on MacArthur-Horn equations to estimate LAI and LAI derived metrics. Compared to the other two metric types, voxel-based metrics offer volumetric estimations of the variation in vegetation density and leaf area throughout the canopy (Almeida et al., 2019a). Voxel matrices contain the distribution of LiDAR returns captured by stacked voxels, which are units of canopy volume (Almeida et al., 2019c). Here, we computed voxels of 1 m^3 based on the MacArthur-Horn equation with the leafR package in R and summed the voxels per unit ground area (1 m^2) to obtain the estimated LAI per unit ground area (MacArthur and Horn, 1969; Almeida, 2021a). We extracted the voxel-based metrics from all three-dimensional voxel matrices within each plot: mean and SD of understory LAI, leaf area height volume (LAHV), and foliage height diversity (FHD) (visual overview in Supplementary Materials D). In a forest, leaf area controls primary productivity (photosynthesis) and is a useful indicator of structural layering in the canopy (Asner et al., 2003). LAI is the leaf area per unit ground area, and is a frequently used metric to assess forest productivity and canopy cover (Asner et al., 2003). LAI understory is the leaf area in the understory of the forest. In this study, we considered vegetation up to 5 m understory. LAHV is an indicator of average vegetation volume and is a useful metric for biomass estimations and for assessing forest function. FHD is a measure of structural diversity and can predict some of the variation in biomass growth in forests.

2.4. Data analysis

Many of the 33 metrics described height levels in the canopy, especially the height percentiles, with potentially high correlation. To prevent overfitting and improve model stability, we removed the highly correlated input metrics (Shi et al., 2018b). To select metrics, we used Pearson's r correlation coefficient to select the strongest correlating metrics and we applied the Boruta algorithm to determine a ranking based on Mean Decrease Accuracy (MDA). For the metrics with a correlation coefficient of $r > 0.9$, we removed the metric(s) with the lower MDA value. Hereafter, we continued the analysis with 18 metrics: mean

CHM, canopy rugosity, gap fraction, hp10SD, hp50SD, dq60mean, dq80mean, dq20SD, dq40SD, dq60SD, dq80SD, Cminmean, GC, LAI mean, LAI SD, LAI understory, LAHV, and FHD. The metrics dqimean and dqiSD are the cloud return density mean and cloud return density variation of the ith percentile, respectively. hpiSD is the variation in height of the ith percentile. Next, we created a biplot with a PCA scoring plot and a corresponding plot of the loadings of variables to assess how the six types were associated with the 18 LiDAR -derived structural metrics.

To distinguish the forest types using the LiDAR metrics with a supervised classification approach, we defined two classification problems. One was to classify the forest plots into six classes in line with the six types. The other was to classify the plots into two simplified types: conservation forest and production forest (section 2.2). For both cases, we used the RF algorithm. RF is a non-parametric machine learning algorithm with internal cross-validation that uses several decision trees to make predictions for classification and regression (Belgiu and Drăguţ, 2016). Additionally, the algorithm handles high data dimensionality well and is insensitive to multicollinearity, data noise, outliers, and overfitting (Belgiu and Drăguţ, 2016).

For the supervised classification of the six types, we tested different combinations of the RF parameters 'Ntree' and 'Mtry' in classification with all 18 metrics. We continued with the parameter values that produced the highest overall classification accuracy. Then, to find the most important metrics for the classification problem and to keep the model as simple as possible, we reduced the number of metrics based on the importance value. The importance value was calculated as the mean increase in the MDA divided by its SD for each metric, as implemented in the Caret package (Kuhn, 2008). The greater the decrease in accuracy of the classifier due to the removal of a single metric, the more important that metric is to the model (Liu et al., 2017). To optimize the supervised classification model, we removed the metric with the lowest importance value from the model, until the model accuracy stabilized with the lowest number of metrics. This process has been shown to reduce the number of less relevant predictors and has been successful in several classification problems (Belgiu and Drăguţ, 2016). The metrics in the final model were thus the most important for the supervised classification of the six types. We calculated their importance values to further quantify the added value of the most important metrics in classification. We applied the same process of parameter tuning and metric removal to the groups classification (simplified model) to get a final supervised RF classification model with the most important metrics.

Due to the large differences in sample sizes between types (section 2.1) the data is unbalanced. During training of RF models, there can be learning problems with unbalanced data, because RF is developed to minimize the overall error rate and will tend to focus more on the majority class in the data (Chen and Breiman, 2004). We chose Leave One Out Cross Validation (LOOCV) to make best use of all samples in the sample sets with the lowest number of samples and minimize the bias from training RF with the unbalanced data. Although LOOCV will not avoid biases, making the best use of the training data affects the classification accuracy the least. LOOCV is a special type of k-fold cross validation technique. LOOCV splits the data into training and validation sets by using all but one sample for training the model and using one sample for validating the model. This process is repeated until all samples have been used once for validating the model.

We assessed the performance of the six typologies and simplified group model to answer how accurately the types could be classified. We built a confusion matrix with the test data predictions and calculated the Producer's Accuracy (PA), User's Accuracy (UA), and Overall Accuracy (OA) (Xu et al., 2015). Besides these performance metrics, we used the mean LOOCV overall accuracy. We used the same metrics and confusion matrix to assess the simplified groups model. We used the ranked importance values for the metrics, as described in section 2.5.3, in both the classification models to answer which metrics were most effective in classification.

The variables that were used in the final models were statistically analyzed. For the six type model, we used nonparametric Kruksal-Wallis tests and Dunn's post hoc tests to test the differences between groups for each variable. For the simplified model, we used nonparametric Mann-Whitney *U* tests. All analyses were performed in R (R Core Team R Foundation for Statistical Computing, 2022).

3. Results

3.1. Supervised classification performance assessment

The classification model for the six types resulted in a LOOCV mean accuracy of 62% (Table 4). The overall accuracy calculated from the collective outcomes was 62% too. Monoculture plantation was better classified than the other types, with both the highest UA (78.8%) and PA (85.2%), however, it was least distinguishable from abandoned monoculture, with 8% of the plots wrongly classified as that category. Restoration plantation was the second best classified, but had 17% of plots wrongly classified as second-growth forest. Next, 54% of second-growth forest was correctly classified, while 33% of these plots were wrongly classified as restoration plantation. Thus, second-growth forest and restoration plantation were difficult to distinguish from each other. Many of the abandoned monoculture plots were classified in their original (post management) state as monoculture plantation (50%), and just 25% were correctly classified as abandoned. Forest remnants were classified with a very low accuracy, and appeared very difficult to distinguish from abandoned monoculture, second-growth forest and restoration plantation. Lastly, mixed plantation was not accurately classified, and was frequently confused with monoculture plantation (38%) and abandoned monoculture (38%).

The simplified classification model (Conservation vs. Production) resulted in a LOOCV mean accuracy of 89% (Table 5). The overall accuracy calculated from the collective outcomes was 90%. In the simplified classification, both groups were classified with higher accuracy than the six types model. Conservation plots were classified as production plots 8% of the time and production plots were classified as conservation plots 11% of the time.

3.2. Importance of the supervised classification metrics

First, we assessed how the forest types were associated with the LiDAR-derived structural metrics (Fig. 4). The first principal component of the three clusters accounts for 31.55% of the total variance, and was formed mainly by height metrics: LAHV, hp10SD and hp50SD, CHM mean, Cminmean, and Gini index. The second principal component accounted for 25.51% of the total variance, and was a "cloud density and leaf area variation" axis, with highest loadings on dq60mean, dq80mean, dq60SD, dq80SD, FHD and LAI SD.

From the RF classification, LAI understory showed the most effective metric in both six types and simplified classification models (Fig. 5).

In the six types model, three predictors were left over after the variable reduction (LAI understory, canopy rugosity, and dq60SD). LAI understory displayed the highest variation between all types (Figs. 6, 7) and was the most important variable for classifying monoculture plantation, restoration plantation, and second-growth forests . In the simplified model, two predictors were left over after variable reduction (LAI understory and hp50SD).

Canopy rugosity was the second most important metric in the six types classification. It was important for the classification of abandoned monoculture, second-growth forests, and restoration plantation. In the simplified classification, the high plantation hp50SD values showed a clear distinction with the low natural type values (Fig. 7).

Variation in vegetation density in the upper half of the forest plot (dq60SD) had very similar ranges for all types (Fig. 6). Nevertheless, the different mean values indicate this metric was useful in distinguishing types within the natural group and plantation group types. Lastly,

Table 4

Confusion matrix for classification of six types with User's Accuracy (UA), Producer's Accuracy (PA), and overall accuracy. The correctly classified plots are in bold.

		Predicted						
		Forest remnant	Second-growth forest	Restoration plantation	Mixed plantation	Abandoned monoculture	Monoculture plantation	PA (%)
Reference	Forest remnant	**0**	2	1	0	4	0	0.0
	Second-growth forest	1	**13**	8	0	2	0	54.2
	Restoration plantation	0	5	**23**	0	1	1	76.7
	Mixed plantation	1	0	1	**0**	3	3	0.0
	Abandoned plantation	1	2	1	1	**5**	10	25.0
	Monoculture plantation	0	2	2	0	5	**52**	85.2
	UA (%)	0.0	54.2	63.9	0.0	25.0	78.8	62.0

Table 5

Confusion matrix for classification of the clustered types with User's Accuracy (UA), Producer's Accuracy (PA), and overall accuracy. The correctly classified plots are in bold. Conservation contained forest remnant, second-growth forest and restoration plantation. Production contained mixed plantation, abandoned monoculture and monoculture plantation.

		Predicted		
		Conservation	Production	PA (%)
Reference	Conservation	**56**	5	91.8
	Production	10	**79**	88.8
	UA (%)	84.8	94.0	90.0

regarding canopy rugosity, ecological restoration plantation had the lowest mean value and abandoned monoculture the highest, which made them stand out from the others.

4. Discussion and conclusions

In this study, we explored the potential of UAV-LiDAR-derived metrics to distinguish six tropical forest restoration types that differ in their conservation and production value in landscapes undergoing restoration. We found that the conservation and production groups could be classified with high accuracy (90%), however, classifying the six forest types separately resulted in medium accuracy (62%). LAI understory, canopy rugosity and a metric that expressed horizontal variability of plot point clouds (dq60SD) were most important in distinguishing types.

4.1. Distinction of types with supervised classification

We found that forest types could be distinguished with high accuracy (90%) while using a simplified model in which the types were grouped in a conservation and a production group (Table 5). However, forest types could only be distinguished with moderate accuracy (62%) when the six types were in separate classes (Table 4). In both, the six types and simplified classification model, the metric LAI understory (voxel derived metric) was most important (Figs. 6, 7). The other important predictors, canopy rugosity (CHM derived metric) and the variation in vegetation density in the upper half of the forest plot (dq60SD, point cloud statistic) in the six types classification and hp50SD (point cloud statistic) in the
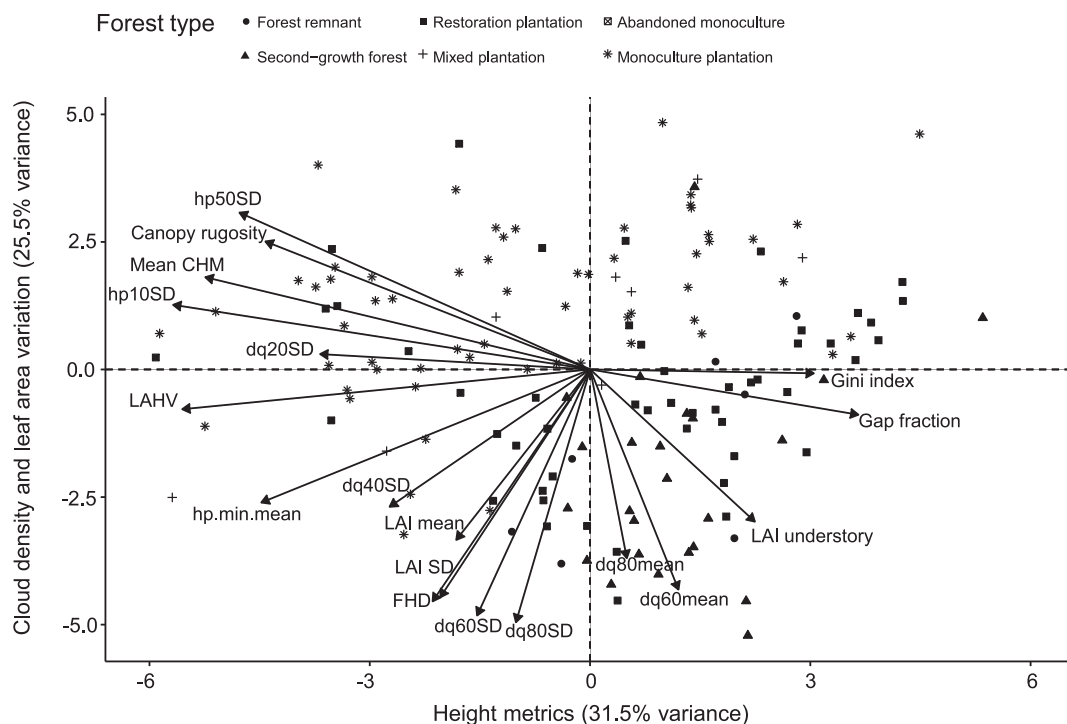

Fig. 4. Biplot of all data points on the first and second Principal Component analysis (PCA) axes. The true types are indicated by shapes. The axes were named by the metrics that had the highest loadings on that PCA component.
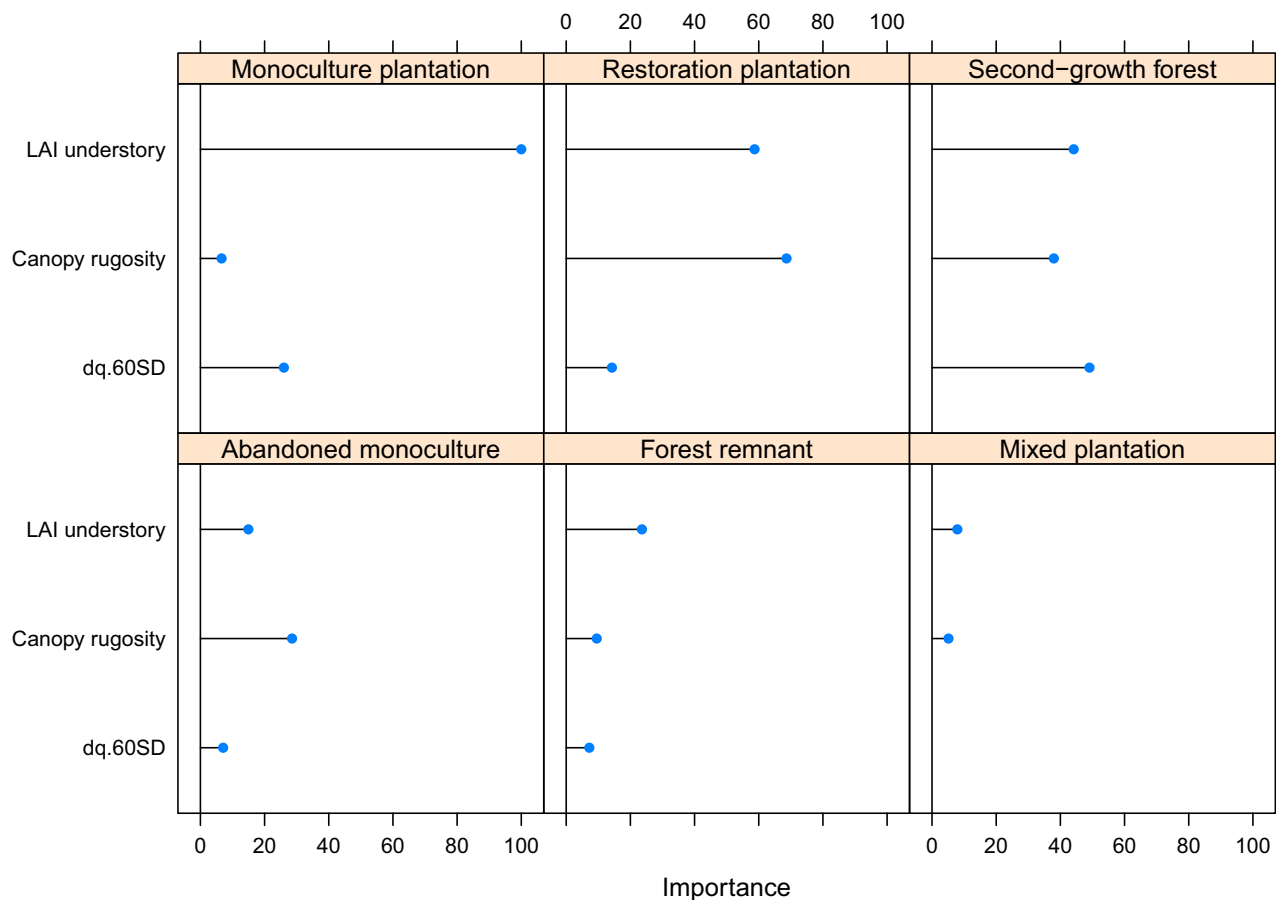
Fig. 5. The variable importance values of the three metrics in the six types model per forest type, sorted from largest importance to lowest. The importance is the mean increase in MDA divided by its SD.

simplified model, were based on horizontal variation in vegetation structure. These three metrics reflected how dissimilar the horizontal vegetation distribution is at small distances at different heights in the forest stand. This corresponds with the loadings in the PCA biplot, where the vectors of the selected classification metrics show either negative correlation (angle close to 180 degrees) or close to no correlation (angle close to 90 degrees) (Fig. 4). Below we discuss the four metrics that were important to distinguish the forest types.

LAI understory. LAI understory was the most important predictor for the six type model and the simplified model. Monoculture plantations consistently had the lowest understory values and therefore were the best-classified. Abandoned monoculture plantations were generally misclassified for monoculture plantations, which may have been caused by whether abandoned monoculture plantations were abandoned before or after harvest of the production species (Chazdon and Guariguata, 2016). Second-growth forests and restoration plantation plots had a similar range in LAI understory values, but the mean was higher for second-growth forests (Fig. 6). Approximately 17% of restoration plantation plots were misidentified as second-growth forest plots and 33% of second-growth forest plots were misidentified as restoration plantation plots (Table 4). Restoration plantations can have less regenerating vegetation in the understory than second-growth forests, due to both local and landscape inhibitors of establishment and the design of the restoration plantations (César et al., 2018). For understanding the effect of restoration efforts and costs, it is especially important to distinguish second-growth forest and restoration plantations (Molin et al., 2018). Although forest remnants and mixed plantations performed poorly in the six type model (for both PA = 0%), they were predominantly classified in line with the conservation and production groups,

respectively. Their poor performance is most likely due to the low sample sizes of both types.

The LAI understory findings in our study clearly reflect the differences between even-aged, regular spaced, and managed tree plantations on the one hand, and naturally regrowing types with little to no management on the other hand. Typically, tree plantations are managed so that there is no understory and only regeneration of the planted species. Although restoration plantations are planted, their management typically differs in that understory vegetation is allowed to grow there. Findings by Almeida et al. (2019b) support that LAI understory is important to characterize and distinguish tropical restoration forests where monoculture tree plantations were classified accurately (100%). Tymen et al. (2017) also confirmed that distinction of forest types by understory is important, because there are consistent micro-environmental differences in forest types. However, in general, the estimation of the understory with LiDAR has received little attention (Wing et al., 2012). A certain pulse density, penetration, and sensor sensitivity are needed to properly estimate understory vegetation, especially with dense canopy covers such as in tropical forests, which have only become available recently. Almeida et al. (2019a) recommended that a point density of at least 15 points m^{-2} is needed for a reasonable LAD estimation to compute LAI. Still, this point density leaves a noteworthy amount of variation in understory volume unexplained (Campbell et al., 2018). Densities of at least 170 points m^{-2} would be necessary to identify understory tree crowns in a mixed forest (Campbell et al., 2018). Furthermore, Almeida et al. (2019c) and Silva et al. (2017) found that for vegetation structural attributes the bias for estimating LAD is small after 20 points/m^2 and further decreases with increasing pulse density, and that estimating canopy heights stabilize
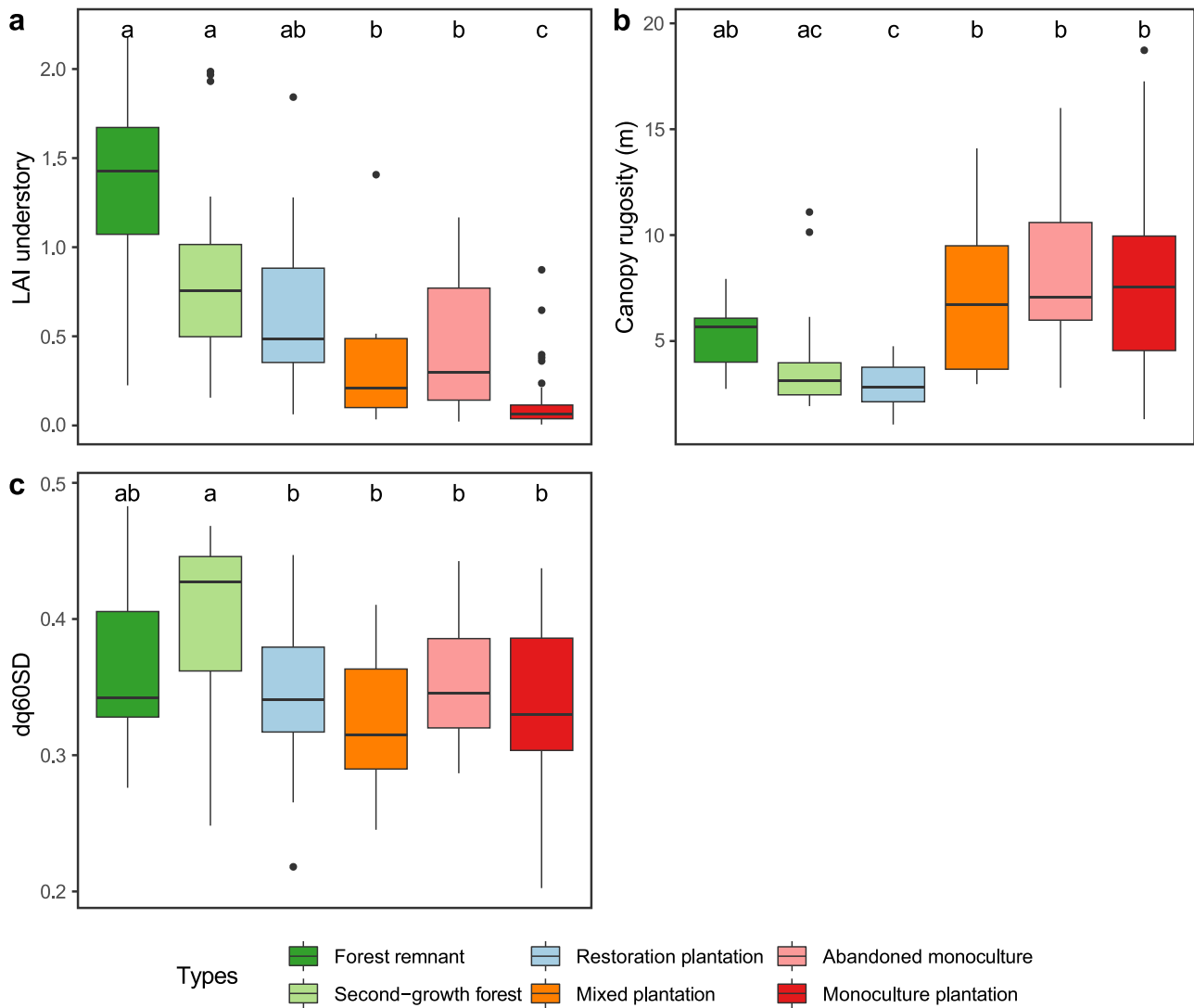
Fig. 6. Boxplots of the three metrics used in the six types model after variable reduction in order of importance: (a) LAI understory; (b) canopy rugosity; (c) variation in vegetation density in the upper half of the forest plot (dq60SD). The statistical analyses consisted of nonparametric Kruksal-Wallis H tests with Dunn's post hoc tests to determine which forest types are different.

after 4 points/m². In this study, the average point densities ranged between 80 and 300 points m^{-2} (Table 2), which proved to be sufficient for a volume estimation of understory and indicates that the effect of the variation of point densities and point spacing (Table 2) between plots is small. In general, it is important to note a limitation that LAI understory derived from LiDAR only indicates the volume of understory vegetation, but nothing about the quality or diversity of the understory community. After large disturbances (like a harvest), lianas or invasive species can completely overgrow the cleared area and can lead to a permanently degraded state that will only change with the help of active management (Chazdon and Guariguata, 2016).

Canopy rugosity. Many LiDAR metrics are often focused on vertical structure or variation, while specific horizontal heterogeneity is rarely addressed (Hardiman et al., 2018). Canopy rugosity is more frequently used (Almeida et al., 2019b; Camarretta et al., 2020a), but only captures variation in the top of the canopy. For canopy rugosity (and hp50SD, see below) the higher SD values can be explained by the regular spacing of even-aged plantation trees, which is a typical characteristic for the production types (Fig. 6). For the conservation types, lower SD values indicate a more constant and homogeneous distribution of vegetation in the horizontal space.

dq60SD. Our results showed that the dq60SD height metric in the six

type model, which represents the variation in vegetation density in the 60th height percentile of the forest plots, was the least differentiating metric of the metrics included in the models (Fig. 6). Although not as clear as canopy rugosity, dq60SD also divided the six types into two groups: planted trees (including restoration plantation) vs non-planted trees (forest remnant and second-growth forest). In contrast to canopy rugosity and hp50SD, the planted tree types showed less variation compared to the non-planted tree types. This contrast can be explained by the different vertical vegetation distributions of the six types. Typically, non-planted types are more likely to have equally distributed vertical vegetational structure and thus the proportion of return point density above the 60th percentile tends to have more variation. This is also in line with the differences in LAI understory. In contrast, planted types are more homogenous where vertical vegetational structure is more concentrated (typically in the canopy). Previous studies have found that these proportions of return point densities can be used to identify structural layers in heterogeneous forests and capture structural attributes (Cao et al., 2014; Maltamo et al., 2005).

hp50SD. The metric hp50SD in the simplified classification model, which represents the horizontal variation of the average height at the 50th percentile, captures subcanopy vegetation variation. Similar to canopy rugosity, the higher SD values of hp50SD can be explained by the
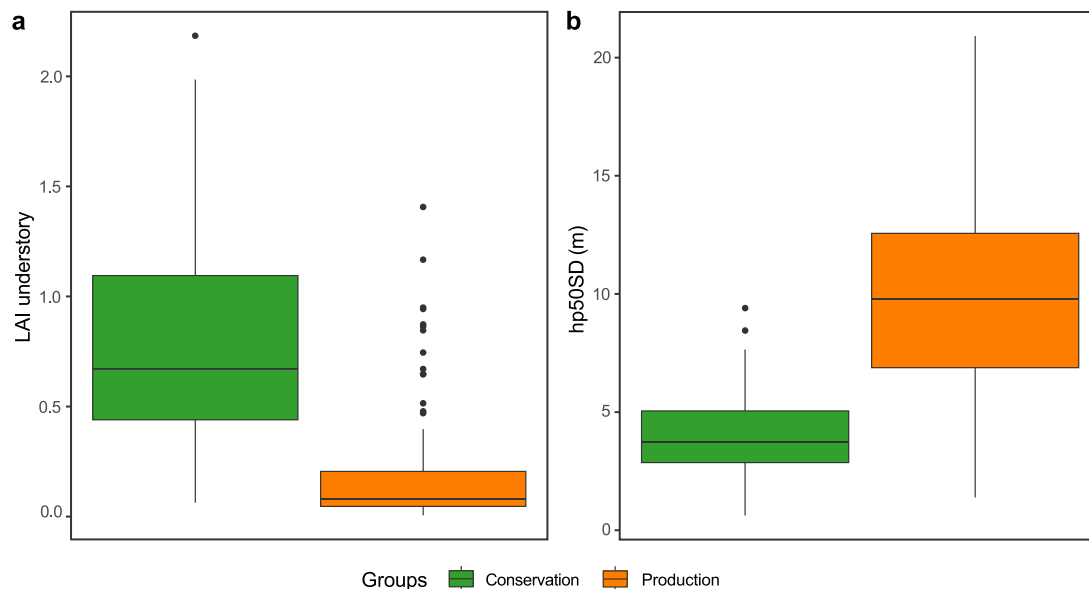
Fig. 7. Boxplots of the two metrics in the clustered type model after variable reduction in order of importance: (a) LAI understory; (b) hp50SD. The statistical analyses consisted of nonparametric Mann-Whitney U tests. Conservation forest and production forest differed significantly from each other for the model metrics LAI understory ($P < .001$, $N_{conservation} = 61$, $N_{production} = 89$) and hp50SD ($P < .001$, $N_{conservation} = 61$, $N_{production} = 89$).

regular spacing of even-aged plantation trees and lower SD values indicate a more constant and homogeneous distribution of vegetation in the horizontal space. There are no studies that used such SD metrics at a similarly small grid size (0.25 m). With a larger grid size, the pattern may have been reversed, as Almeida et al. (2019b) found. Robinson et al. (2018), in a tropical forest in Costa Rica, found that the SD of the 25th height percentile could predict species richness. Moreover, Hardiman et al. (2018) showed that spatial variation in canopy structure metrics may reflect important processes between forest types and landscapes. Therefore, such variation metrics could be of use in restoration monitoring.

In summary, differences in vegetation structure between conservation and production types clearly reflect differences in management. Active management in production types, including the removal or suppression of understory vegetation (although not for abandoned monocultures) and the planting of trees in rows, leads to a very different forest structure than management allowing for naturally regenerated forest (Chazdon and Guariguata, 2016). Distinguishing these two groups is important at a landscape scale: in large scale restoration initiatives or general forest assessments, forest cover has been the primary indicator with no distinction between natural and planted forests (Almeida et al., 2019b; Chazdon et al., 2016), even while these forests differ significantly in ecological functioning, biodiversity and the provisioning of services (Chazdon, 2008).

For successful classification of forest types, the variation in structure within types should be less than the maximum variation between types captured by the high-resolution LiDAR metrics (Shi et al., 2018a). In addition, the low number of samples in the forest remnant and mixed plantation types, and therefore imbalanced classes, may have contributed to the low classification accuracies in the six type model. The difference in classification success between both models underlines the difficulty of distinguishing individual forest types that are very similar in management, regeneration dynamics, and structure. However, more noise was added to the classes, due to plots with different ages and with different tree species, which may have increased the heterogeneity of studied areas. Alternatively, when grouped by management and growth form type, the simplified conservation and production types were sufficiently different in structure to result in high classification accuracies.

4.2. Monitoring forest restoration outcomes with remote sensing

Successful monitoring of forest restoration, especially given the international ambitions to restore hundreds of millions of hectares of forest, requires more than upscaling conventional field inventory efforts (de Almeida et al., 2019; Camarretta et al., 2020). On the one hand, field inventories provide detailed information but are costly and time intensive. Alternatively, space-borne platforms are largely unable to provide the detail of information necessary to assess the success of forest restoration. Considering this gap, we believe that UAV-borne LiDAR can address the need for detailed information while upscaling monitoring efforts to meet the needs of large scale forest restoration. Below, we discuss the potential use of this study's approach.

Optimizing monitoring efforts. Our results and the results of other studies (e.g. Almeida et al., 2021; d'Oliveira et al., 2020) with similar systems and approaches showed that UAV-borne systems have a large potential to optimize forest restoration monitoring efforts in terms of costs and scalability. Although the initial investments to set up a UAV system are relatively high, the system is very flexible to use and can cover large areas in a day (up to 1000 ha) while collecting detailed data (e.g. structural attributes, functional attributes, diversity). Furthermore, pre-stratification of the structural attributes based on UAV-LiDAR can help to set up in situ plots for monitoring to cover the greatest variety in vegetational structure and at the same time reduce the number of plots needed by up to 41% (Papa et al., 2020).

Assess structural attributes. UAV-LiDAR has the potential to measure structural attributes that are more difficult to measure with field campaigns, but contribute to restoration targets nonetheless (Camarretta et al., 2020). For example, LAI understory is difficult and laborious to assess in the field, however, UAV-LiDAR can quantify this metric and can support practitioners with adaptive management interventions. Furthermore, measuring structural attributes with UAV-LiDAR can provide more accurate results compared to in situ measurements, for example, to estimate tree height or gap dimensions (d'Oliveira et al., 2020).

Our results have shown that high-density discrete return UAV-LiDAR can identify detailed structural characteristics to distinguish broad tropical forest types, however, these structural characteristics alone were not enough to fully separate similar forest types. Part of this limitation may result from the assessment of plots with different ages and

with different tree species, which may increase the heterogeneity of studied areas. In general, more research is needed to deploy the full potential of UAV-borne monitoring in forest restoration. Here, we discuss a few potential steps forward.

Fusion LiDAR and optical sensors. For further distinction of similar types, and avoiding noise from different successional stages and forest age, future research could explore LiDAR fusion with optical sensors. While LiDAR captures forest structure, optical sensors can be complementary by providing information about the spectral signatures of the forest. For example, hyperspectral imagery has shown great potential for distinguishing vegetation classes and species, including features like alpha and beta diversity (Féret and Asner, 2012, 2014).

Distinguish successional stage. In addition to increasing the classification accuracy by fusing LiDAR and optical sensors, there is a need to distinguish the successional stage of plots within forest types with UAV-borne monitoring systems. The successional stage of forest types change over time (such as species composition and structural attributes), but the same successional stages of different forest types may look very similar in terms of structure (e.g. basal area) and, therefore, increase the difficulty of distinguishing them with LiDAR alone. Therefore, to increase the accuracy, one possible improvement would be to stratify classification by successional stages or to make a model that predicts both successional stage and forest type (Leutner et al., 2012). After this, it is possible to make the step towards actual monitoring and identifying which metrics are most relevant to track progress. Another potential option is to include very high resolution images (e.g. UAV-RGB) to identify tree species which are indicators of successional stage (Ferreira et al., 2020; Wagner et al., 2019).

Accessibility to technology. To deploy UAV-based monitoring, it is crucial to have access to the financial resources to invest in the upfront costs of UAV monitoring systems and train people on how to use these systems and perform the analyses. In many tropical countries, high costs can be a bottleneck (e.g. high import tariffs and disadvantageous currency exchange rates) and technical assistance can be lacking. Fortunately, UAV-based systems become more affordable and software packages and training are open source and freely available.

Spaceborne LiDAR. Furthermore, NASA's recent spaceborne Global Ecosystem Dynamics Investigation (GEDI) platform may have the potential to increase the spatial coverage compared to UAV-LiDAR systems. However, accuracy and precision are lower, and the GEDI system only samples a limited portion of Earth's land surface (Dubayah et al., 2020).

In conclusion, given the unprecedented scale of global forest restoration efforts, UAV-LiDAR, potentially in combination with other sensors and remote sensing systems, has a huge potential to meet the needs of monitoring landscapes under restoration by its ability to collect detailed information over large spatiotemporal scales, reduce costs and sampling efforts, inform stakeholders about the progress of restoration success and guide adaptive management where needed. This study highlighted that UAV-LiDAR can efficiently identify structural differences in a broad range of forest restoration sites in the tropics and therefore can play a critical role in forest restoration monitoring and in the accountability of restoration initiatives.

CRediT authorship contribution statement

Janneke Scheeres: Conceptualization, Methodology, Software, Validation, Formal analysis, Investigation, Writing – original draft, Writing – review & editing, Visualization. **Johan de Jong:** Conceptualization, Methodology, Formal analysis, Writing – original draft, Writing – review & editing, Visualization. **Benjamin Brede:** Conceptualization, Methodology, Validation, Writing – original draft, Writing – review & editing. **Pedro H.S. Brancalion:** Conceptualization, Methodology, Investigation, Writing – original draft, Writing – review & editing, Supervision, Project administration, Funding acquisition. **Eben Noth Broadbent:** Investigation, Writing – review & editing, Resources, Data

curation. **Angelica Maria Almeyda Zambrano:** Investigation, Writing – review & editing, Resources, Data curation. **Eric Bastos Gorgens:** Writing – review & editing, Resources, Data curation. **Carlos Alberto Silva:** Writing – review & editing, Resources, Data curation. **Ruben Valbuena:** Writing – review & editing, Resources, Data curation. **Paulo Molin:** Investigation, Resources, Data curation, Writing – review & editing, Supervision, Project administration. **Scott Stark:** Conceptualization, Writing – review & editing. **Ricardo Ribeiro Rodrigues:** Writing – review & editing, Supervision, Project administration. **Giulio Brossi Santoro:** Investigation, Resources, Data curation, Writing – review & editing. **Angélica Faria Resende:** Investigation, Data curation, Writing – review & editing, Project administration. **Catherine Torres de Almeida:** Investigation, Data curation, Writing – review & editing, Supervision, Project administration. **Danilo Roberti Alves de Almeida:** Conceptualization, Methodology, Investigation, Data curation, Writing – original draft, Writing – review & editing, Supervision, Project administration.

Declaration of Competing Interest

The authors declare that they have no known competing financial interests or personal relationships that could have appeared to influence the work reported in this paper.

Data availability

Data will be made available on request.

Acknowledgments

Appendix A. Supplementary data

Supplementary data to this article can be found online at https://doi.org/10.1016/j.rse.2023.113533.

References

Almeida, D.R.A., Broadbent, E.N., Zambrano, A.M.A., Wilkinson, B.E., Ferreira, M.E., Chazdon, R., Meli, P., Gorgens, E.B., Silva, C.A., Stark, S.C., Valbuena, R., Papa, D.A., Brancalion, P.H.S., 2019a. Monitoring the structure of forest restoration plantations with a drone-lidar system. Int. J. Appl. Earth Obs. Geoinf. 79, 192–198. https://doi.org/10.1016/j.jag.2019.03.014.

Almeida, D.R.A., Stark, S.C., Chazdon, R., Nelson, B.W., Cesar, R.G., Meli, P., Gorgens, E. B., Duarte, M.M., Valbuena, R., Moreno, V.S., Mendes, A.F., Amazonas, N., Gonçalves, N.B., Silva, C.A., Schietti, J., Brancalion, P.H.S., 2019b. The effectiveness of lidar remote sensing for monitoring forest cover attributes and landscape restoration. For. Ecol. Manag. 438, 34–43. https://doi.org/10.1016/j.foreco.2019.02.002.

Almeida, Danilo Roberti Alves, Stark, S.C., Shao, G., Schietti, J., Nelson, B.W., Silva, C.A., Gorgens, E.B., Valbuena, R., Brancalion, P.H.S., Papa, D., 2019. Optimizing the remote detection of tropical rainforest structure with airborne lidar: leaf area profile sensitivity to pulse density and spatial sampling. Remote Sens. (Basel) 11, 92. https://doi.org/10.3390/rs11010092.

de Almeida, D.R., Stark, S.C., Valbuena, R., Broadbent, E.N., Silva, T.S., de Resende, A.F., Brancalion, P.H., 2019d. A new era in forest restoration monitoring. Restor. Ecol. 28 (1), 8–11. https://doi.org/10.1111/rec.13067.

Almeida, D.R.A., 2021a. LeafR: Provides a set of functions for analyzing the ecological structure of forests based on lai and lad measures derived from lidar data [R package version 0.3.5].

Almeida, D.R.A., Broadbent, E.N., Ferreira, M.P., Meli, P., Zambrano, A.M.A., Gorgens, E.B., Resende, A.F., Almeida, C.T., Amaral, C.H., Corte, A.P.D., Silva, C.A., Romanelli, J.P., Prata, G.A., Almeida Papa, D., Stark, S.C., Valbuena, R., Nelson, B.W., Guillemot, J., Féret, J.-B., Chazdon, R., Brancalion, P.H.S., 2021. Monitoring restored tropical forest diversity and structure through UAV-borne hyperspectral and lidar fusion. Remote Sens. Environ. 264, 112582 https://doi.org/10.1016/j.rse.2021.112582.

Asner, G.P., Scurlock, J.M.O., Hicke, A., J., 2003. Global synthesis of leaf area index observations: implications for ecological and remote sensing studies. Glob. Ecol. Biogeogr. 12, 191–205. https://doi.org/10.1046/j.1466-822X.2003.00026.x.

Belgiu, M., Drăguţ, L., 2016. Random forest in remote sensing: a review of applications and future directions. ISPRS J. Photogramm. Remote Sens. 114, 24–31. https://doi.org/10.1016/j.isprsjprs.2016.01.011.

Brancalion, P.H.S., Niamir, A., Broadbent, E., Crouzeilles, R., Barros, F.S.M., Almeyda Zambrano, A.M., Baccini, A., Aronson, J., Goetz, S., Reid, J.L., Strassburg, B.B.N., Wilson, S., Chazdon, R.L., 2019. Global restoration opportunities in tropical rainforest landscapes. Sci. Adv. 5, eaav3223. https://doi.org/10.1126/sciadv.aav3223.

Camarretta, N., Harrison, P.A., Bailey, T., Potts, B., Lucieer, A., Davidson, N., Hunt, M., 2020. Monitoring forest structure to guide adaptive management of forest restoration: a review of remote sensing approaches. New Forest 51, 573–596. https://doi.org/10.1007/s11056-019-09754-5.

Campbell, M.J., Dennison, P.E., Hudak, A.T., Parham, L.M., Butler, B.W., 2018. Quantifying understory vegetation density using small-footprint airborne lidar. Remote Sens. Environ. 215, 330–342. https://doi.org/10.1016/j.rse.2018.06.023.

Cao, L., Coops, N., Hermosilla, T., Innes, J., Dai, J., She, G., 2014. Using small-footprint discrete and full-waveform airborne LiDAR metrics to estimate Total biomass and biomass components in subtropical forests. Remote Sens. 6, 7110–7135. https://doi.org/10.3390/rs6087110.

César, R.G., Moreno, V.S., Coletta, G.D., Chazdon, R.L., Ferraz, S.F.B., de Almeida, D.R.A., Brancalion, P.H.S., 2018. Early ecological outcomes of natural regeneration and tree plantations for restoring agricultural landscapes. Ecol. Appl. 28, 373–384. https://doi.org/10.1002/eap.1653.

Chazdon, R.L., 2008. Beyond deforestation: restoring forests and ecosystem services on degraded lands. Science 320, 1458–1460. https://doi.org/10.1126/science.1155365.

Chazdon, R.L., Brancalion, P.H.S., Laestadius, L., Bennett-Curry, A., Buckingham, K., Kumar, C., Moll-Rocek, J., Vieira, I.C.G., Wilson, S.J., 2016. When is a forest a forest? Forest concepts and definitions in the era of forest and landscape restoration. Ambio 45, 538–550. https://doi.org/10.1007/s13280-016-0772-y.

Chazdon, R.L., Guariguata, M.R., 2016. Natural regeneration as a tool for large-scale forest restoration in the tropics: prospects and challenges. Biotropica 48, 716–730. https://doi.org/10.1111/btp.12381.

Chazdon, R.L., Lindenmayer, D., Guariguata, M.R., Crouzeilles, R., Benayas, J.M.R., Chavero, E.L., 2020. Fostering natural forest regeneration on former agricultural land through economic and policy interventions. Environ. Res. Lett. 15 (4), 043002 https://doi.org/10.1088/1748-9326/ab79e6.

Chazdon, R., Norden, N., Colwell, R.K., Chao, A., 2022. Monitoring recovery of tree diversity during tropical forest restoration: lessons from long-term trajectories of natural regeneration. R. Soc. Lond. Phil. Trans. B. Biol. Sci. 378 https://doi.org/10.1098/rstb.2021.0069.

Chen, C., Breiman, L., 2004. Using Random Forest to Learn Imbalanced Data. University of California, Berkeley.

Clark, D.B., Olivas, P.C., Oberbauer, S.F., Clark, D.A., Ryan, M.G., 2008. First direct landscape-scale measurement of tropical rain forest leaf area index, a key driver of global primary productivity. Ecol. Lett. 11 (2), 163–172. https://doi.org/10.1111/j.1461-0248.2007.01134.x.

Crouzeilles, R., Ferreira, M.S., Chazdon, R.L., Lindenmayer, D.B., Sansevero, J.B., Monteiro, L., Strassburg, B.B., 2017. Ecological restoration success is higher for natural regeneration than for active restoration in tropical forests. Sci. Adv. 3 (11), e1701345 https://doi.org/10.1126/sciadv.1701345.

d'Oliveira, M.V., Broadbent, E.N., Oliveira, L.C., Almeida, D.R., Papa, D.A., Ferreira, M.E., Oliveira-da-Costa, M., 2020. Aboveground biomass estimation in Amazonian tropical forests: A comparison of aircraft-and Gatoreye UAV-borne LIDAR data in the Chico mendes extractive reserve in Acre, Brazil. Remote Sens. 12 (11), 1754. https://doi.org/10.3390/rs12111754.

Drake, J.B., Dubayah, R.O., Clark, D.B., Knox, R.G., Blair, J.B., Hofton, M.A., Chazdon, R.L., Weishampel, J.F., Prince, S., 2002. Estimation of tropical forest structural characteristics using large-footprint lidar. Remote Sens. Environ. 79, 305–319. https://doi.org/10.1016/S0034-4257(01)00281-4.

Dubayah, R., Blair, J.B., Goetz, S., Fatoyinbo, L., Hansen, M., Healey, S., Silva, C., 2020. The Global Ecosystem Dynamics Investigation: High-resolution laser ranging of the Earth's forests and topography. Sci. Remote Sens. 1, 100002.

Fang, H., Baret, F., Plummer, S., Schaepman-Strub, G., 2019. An overview of global leaf area index (LAI): methods, products, validation, and applications. Rev. Geophys. 57 (3), 739–799. https://doi.org/10.1029/2018RG000608.

Feng, Y., Schmid, B., Loreau, M., Forrester, D.I., Fei, S., Zhu, J., Fang, J., 2022. Multispecies forest plantations outyield monocultures across a broad range of conditions. Science 376 (6595), 865–868. https://doi.org/10.1126/science.abm6363.

Féret, J.-B., Asner, G.P., 2012. Semi-supervised methods to identify individual crowns of lowland tropical canopy species using imaging spectroscopy and LiDAR. Remote Sens. 4, 2457–2476. https://doi.org/10.3390/rs4082457.

Féret, J.-B., Asner, G.P., 2014. Mapping tropical forest canopy diversity using high-fidelity imaging spectroscopy. Ecol. Appl. 24, 1289–1296. https://doi.org/10.1890/13-1824.1.

Ferreira, M.P., de Almeida, D.R.A., de Almeida Papa, D., Minervino, J.B.S., Veras, H.F.P., Formighieri, A., Ferreira, E.J.L., 2020. Individual tree detection and species classification of amazonian palms using UAV images and deep learning. For. Ecol. Manag. 475, 118397 https://doi.org/10.1016/j.foreco.2020.118397.

Hardiman, B., LaRue, E., Atkins, J., Fahey, R., Wagner, F., Gough, C., 2018. Spatial variation in canopy structure across Forest landscapes. Forests 9, 474. https://doi.org/10.3390/f9080474.

Holl, K.D., Aide, T.M., 2011. When and where to actively restore ecosystems? For. Ecol. Manag. 261 (10), 1558–1563. https://doi.org/10.1016/j.foreco.2010.07.004.

Hua, F., Bruijnzeel, L.A., Meli, P., Martin, P.A., Zhang, J., Nakagawa, S., Balmford, A., 2022. The biodiversity and ecosystem service contributions and trade-offs of forest restoration approaches. Science 376 (6595), 839–844. https://doi.org/10.1126/science.abl4649.

Khosravipour, A., Skidmore, A.K., Isenburg, M., 2016. Generating spike-free digital surface models using LiDAR raw point clouds: a new approach for forestry applications. Int. J. Appl. Earth Obs. Geoinf. 52, 104–114. https://doi.org/10.1016/j.jag.2016.06.005.

Kuhn, M., 2008. Building predictive models in R using the caret package. J. Stat. Softw. 28 https://doi.org/10.18637/jss.v028.i05.

Leutner, B.F., Reineking, B., Müller, J., Bachmann, M., Beierkuhnlein, C., Dech, S., Wegmann, M., 2012. Modelling Forest α-diversity and floristic composition — on the added value of LiDAR plus hyperspectral remote sensing. Remote Sens. 4, 2818–2845. https://doi.org/10.3390/rs4092818.

Lewis, S.L., Wheeler, C.E., Mitchard, E.T., Koch, A., 2019. Restoring natural forests is the best way to remove atmospheric carbon. https://doi.org/10.1038/d41586-019-01026-8.

Liu, L., Coops, N.C., Aven, N.W., Pang, Y., 2017. Mapping urban tree species using integrated airborne hyperspectral and LiDAR remote sensing data. Remote Sens. Environ. 200, 170–182. https://doi.org/10.1016/j.rse.2017.08.010.

Lohbeck, M., Poorter, L., Martínez-Ramos, M., Bongers, F., 2015. Biomass is the main driver of changes in ecosystem process rates during tropical forest succession. Ecology 96 (5), 1242–1252.

Luo, S., Wang, C., Xi, X., Nie, S., Fan, X., Chen, H., Yang, X., Peng, D., Lin, Y., Zhou, G., 2019. Combining hyperspectral imagery and LiDAR pseudo-waveform for predicting crop LAI, canopy height and above-ground biomass. Ecol. Indic. 102, 801–812. https://doi.org/10.1016/j.ecolind.2019.03.011.

MacArthur, R.H., Horn, H.S., 1969. Foliage profile by vertical measurements. Ecology 50, 802. https://doi.org/10.2307/1933693.

Maltamo, M., Packalén, P., Yu, X., Eerikäinen, K., Hyyppä, J., Pitkänen, J., 2005. Identifying and quantifying structural characteristics of heterogeneous boreal forests using laser scanner data. For. Ecol. Manag. 216, 41–50. https://doi.org/10.1016/j.foreco.2005.05.034.

Marselis, S.M., Tang, H., Armston, J., Abernethy, K., Alonso, A., Barbier, N., Dubayah, R., 2019. Exploring the relation between remotely sensed vertical canopy structure and tree species diversity in Gabon. Environ. Res. Lett. 14 (9), 094013 https://doi.org/10.1088/1748-9326/ab2dcd.

Marshall, A.R., Waite, C.E., Pfeifer, M., Banin, L.F., Rakotonarivo, S., Chomba, S., Chazdon, R.L., 2022. Fifteen essential science advances needed for effective restoration of the world's forest landscapes. Philos. Trans. R. Soc. B 378 (1867), 20210065. https://doi.org/10.1098/rstb.2021.0065.

Maxwell, A.E., Warner, T.A., Fang, F., 2018. Implementation of machine-learning classification in remote sensing: an applied review. Int. J. Remote Sens. 39 (9), 2784–2817. https://doi.org/10.1080/01431161.2018.1433343.

Molin, P.G., Chazdon, R., de Barros, Frosini, Ferraz, S., Brancalion, P.H.S., 2018. A landscape approach for cost-effective large-scale forest restoration. J. Appl. Ecol. 55, 2767–2778. https://doi.org/10.1111/1365-2664.13263.

Myers, N., Mittermeier, R.A., Mittermeier, C.G., da Fonseca, G.A., Kent, J., 2000. Biodiversity hotspots for conservation priorities. Nature 403, 853–858. https://doi.org/10.1038/35002501.

Nanni, A.S., Sloan, S., Aide, T.M., Graesser, J., Edwards, D., Grau, H.R., 2019. The neotropical reforestation hotspots: a biophysical and socioeconomic typology of contemporary forest expansion. Glob. Environ. Chang. 54, 148–159. https://doi.org/10.1016/j.gloenvcha.2018.12.001.

Papa, D.A., Almeida, D.R.A., Silva, C.A., Figueiredo, E.O., Stark, S.C., Valbuena, R., Rodriguez, L.C.E., d'Oliveira, M.V.N., 2020. Evaluating tropical forest classification and field sampling stratification from lidar to reduce effort and enable landscape monitoring. Forest Ecol. Manage. 457, 117634 https://doi.org/10.1016/j.foreco.2019.117634.

Poorter, L., Craven, D., Jakovac, C.C., van der Sande, M.T., Amissah, L., Bongers, F., Hérault, B., 2021. Multidimensional tropical forest recovery. Science 374 (6573), 1370–1376. https://doi.org/10.1126/science.abh3629.

R Core Team R Foundation for Statistical Computing, 2022. R: A Language and Environment for Statistical Computing. https://www.r-project.org/.

Robinson, C., Saatchi, S., Clark, D., Hurtado Astaiza, J., Hubel, A., Gillespie, T., 2018. Topography and three-dimensional structure can estimate tree diversity along a tropical elevational gradient in Costa Rica. Remote Sens. 10, 629. https://doi.org/10.3390/rs10040629.

Sankey, T., Donager, J., McVay, J., Sankey, J.B., 2017. UAV lidar and hyperspectral fusion for forest monitoring in the southwestern USA. Remote Sens. Environ. 195, 30–43. https://doi.org/10.1016/j.rse.2017.04.007.

Shi, Y., Skidmore, A.K., Wang, T., Holzwarth, S., Heiden, U., Pinnel, N., Zhu, X., Heurich, M., 2018a. Tree species classification using plant functional traits from LiDAR and hyperspectral data. Int. J. Appl. Earth Obs. Geoinf. 73, 207–219. https://doi.org/10.1016/j.jag.2018.06.018.

Shi, Y., Wang, T., Skidmore, A.K., Heurich, M., 2018b. Important LiDAR metrics for discriminating forest tree species in Central Europe. ISPRS J. Photogramm. Remote Sens. 137, 163–174. https://doi.org/10.1016/j.isprsjprs.2018.02.002.

Silva, C.A., Hudak, A.T., Vierling, L.A., Klauberg, C., Garcia, M., Ferraz, A., Saatchi, S., 2017. Impacts of airborne lidar pulse density on estimating biomass stocks and changes in a selectively logged tropical forest. Remote Sens. 9 (10), 1068. https://doi.org/10.3390/rs9101068.

Silva, C.A., Valbuena, R., Pinagé, E.R., Mohan, M., de Almeida, D.R.A., Broadbent, E.N., Jaafar, W.S.W.M., de Almeida Papa, D., Cardil, A., Klauberg, C., 2019. ForestGapR: An R package for forest gap analysis from canopy height models. Methods Ecol. Evol. https://doi.org/10.1111/2041-210X.13211.

Stark, S.C., Leitold, V., Wu, J.L., Hunter, M.O., de Castilho, C.V., Costa, F.R.C., McMahon, S.M., Parker, G.G., Shimabukuro, M.T., Lefsky, M.A., Keller, M., Alves, L. F., Schietti, J., Shimabukuro, Y.E., Brandão, D.O., Woodcock, T.K., Higuchi, N., de Camargo, P.B., de Oliveira, R.C., Saleska, S.R., Chave, J., 2012. Amazon forest carbon dynamics predicted by profiles of canopy leaf area and light environment. Ecol. Lett. 15, 1406–1414. https://doi.org/10.1111/j.1461-0248.2012.01864.x.

Tymen, B., Vincent, G., Courtois, E.A., Heurtebize, J., Dauzat, J., Marechaux, I., Chave, J., 2017. Quantifying micro-environmental variation in tropical rainforest understory at landscape scale by combining airborne LiDAR scanning and a sensor network. Ann. For. Sci. 74, 32. https://doi.org/10.1007/s13595-017-0628-z.

Valbuena, R., Eerikäinen, K., Packalen, P., Maltamo, M., 2016. Gini coefficient predictions from airborne lidar remote sensing display the effect of management intensity on forest structure. Ecol. Indic. 60, 574–585. https://doi.org/10.1016/j.ecolind.2015.08.001.

Valbuena, R., Maltamo, M., Mehtätalo, L., Packalen, P., 2017. Key structural features of boreal forests may be detected directly using L-moments from airborne lidar data. Remote Sens. Environ. 194, 437–446. https://doi.org/10.1016/j.rse.2016.10.024.

van der Sande, M.T., Poorter, L., Kooistra, L., Balvanera, P., Thonicke, K., Thompson, J., Peña-Claros, M., 2017. Biodiversity in species, traits, and structure determines carbon stocks and uptake in tropical forests. Biotropica 49 (5), 593–603. https://doi.org/10.1111/btp.12453.

van Leeuwen, M., Nieuwenhuis, M., 2010. Retrieval of forest structural parameters using LiDAR remote sensing. Eur. J. For. Res. 129, 749–770. https://doi.org/10.1007/s10342-010-0381-4.

Wagner, F.H., Sanchez, A., Tarabalka, Y., Lotte, R.G., Ferreira, M.P., Aidar, M.P., Aragao, L.E., 2019. Using the U-net convolutional network to map forest types and disturbance in the Atlantic rainforest with very high resolution images. Remote Sens. Ecol. Conserv. 5 (4), 360–375. https://doi.org/10.1002/rse2.111.

Wing, B.M., Ritchie, M.W., Boston, K., Cohen, W.B., Gitelman, A., Olsen, M.J., 2012. Prediction of understory vegetation cover with airborne lidar in an interior ponderosa pine forest. Remote Sens. Environ. 124, 730–741. https://doi.org/10.1016/j.rse.2012.06.024.

Xu, C., Morgenroth, J., Manley, B., 2015. Integrating data from discrete return airborne LiDAR and optical sensors to enhance the accuracy of Forest description: a review. Curr. Forest. Rep. 1, 206–219. https://doi.org/10.1007/s40725-015-0019-3.

Zahawi, R.A., Dandois, J.P., Holl, K.D., Nadwodny, D., Reid, J.L., Ellis, E.C., 2015. Using lightweight unmanned aerial vehicles to monitor tropical forest recovery. Biol. Conserv. 186, 287–295. https://doi.org/10.1016/j.biocon.2015.03.031.

Zolkos, S.G., Goetz, S.J., Dubayah, R., 2013. A meta-analysis of terrestrial aboveground biomass estimation using lidar remote sensing. Remote Sens. Environ. 128, 289–298. https://doi.org/10.1016/j.rse.2012.10.017.